SPATIUM

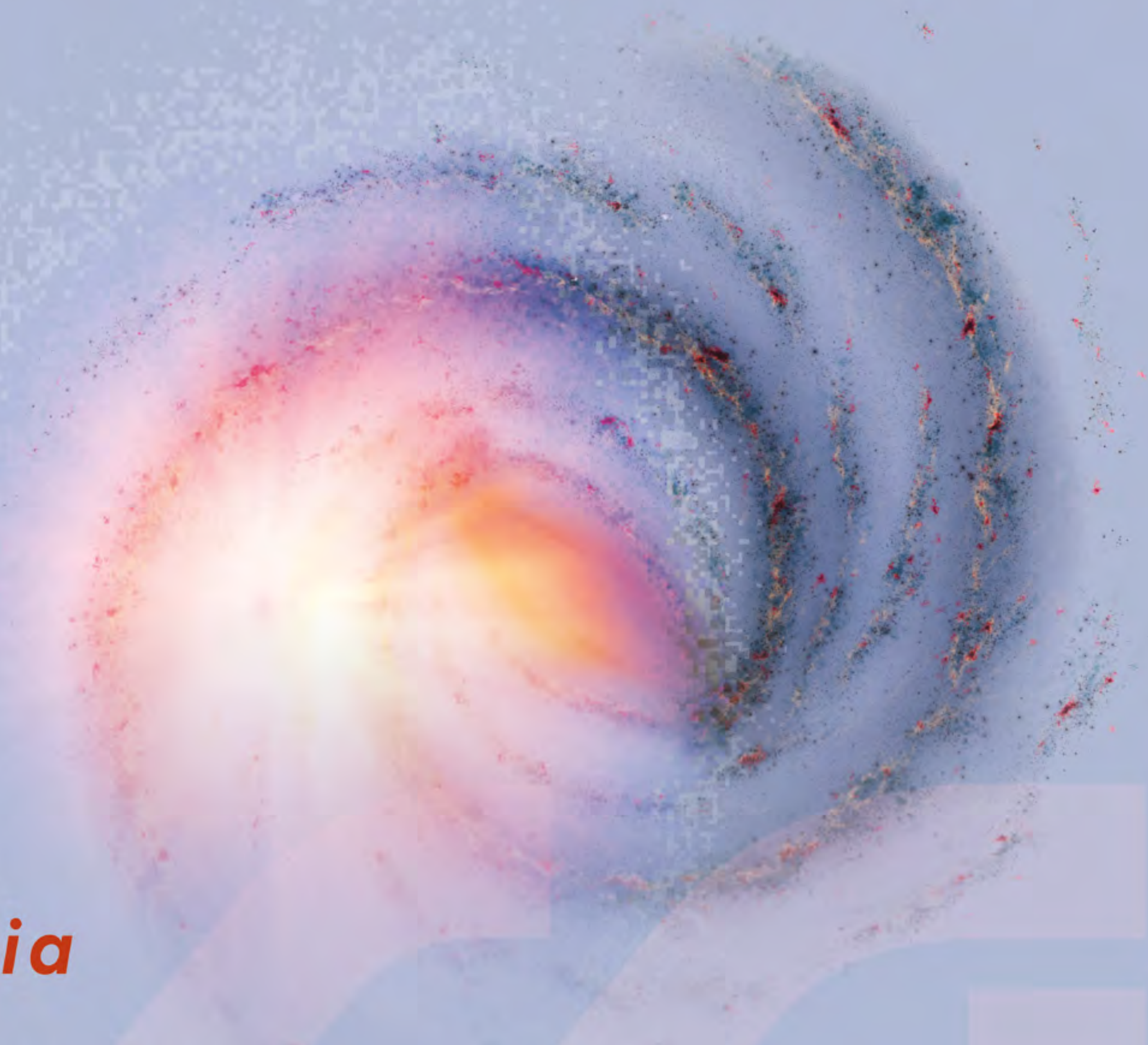

Gaia

The astrometric space observatory that is revolutionising our view of the Milky Way

By Michael Biermann

pro ISSI INTERNATIONAL SPACE SCIENCE INSTITUTE

No. 55, 2024

Published by the Association Pro ISSI

SPATIUM
Published by

Association Pro ISSI
Hallerstrasse 6, CH-3012 Bern
Phone +41 (0)31 684 48 96

see www.issibern.ch/spatium
for the whole SPATIUM series

President
Prof. Dr. Christoph Mordasini
University of Bern

Editor
PD Dr. Andreas Verdun
CH-3086 Zimmerwald

Layout and Design
Fabio Crameri, ISSI Bern

Printing
Länggass Druck AG Bern
CH-3001 Bern

Cover
Spatial distribution of the stars from which the formation history of the Milky Way was determined (after Chandra et al., 2023), superimposed on a artistic schematic image of a spiral galaxy (NASA/JPL–Caltech/R. Hurt).

Editorial

Astrometry is the science of measuring star positions and their motions and of providing star catalogues [11]. Star catalogues and so-called fundamental catalogues [5] were constructed mainly for "materializing" reference frames used in astronomy and geodesy ([4], [9], [16], [18]), and for investigating the structure of the Milky Way by statistical methods ([12], [17]). The famous Bonner Durchmusterung was the last catalogue based on human eye observations, followed by the era of photographic catalogues and surveys, including radio sources ([4], [18]). Since the first decade of the space age, the idea of telescopes in space ([8], [15]) and the development of Charge-Coupled Devices (CCDs) since 1969 [2] became game changers. The impact of Hipparcos (HIgh Precision PARallax COllecting Satellite) on solar system and galactic astronomy was a first step [14]. Space-based astrometry provided new observations relevant in astrophysics as well [10]. The study of galactic structure, kinematics, and dynamics was no longer a theoretical discipline ([3], [13]). The determination of high precision stellar parallaxes (distances) using space borne astrometric observations was the key for any further progress in astronomy, astrophysics, and even cosmology ([6], [19]). Micro-arcsecond astrometry used for determining more precise distances opened new perspectives for astrophysics ([1], [7]). But with the ESA mission Gaia not only the composition, structure, and dynamics of the galaxy become measurable with unprecedented accuracy, but also the modelling of stellar evolution represented by the Hertzsprung-Russell-Diagram (HRD) was raised to a new level of precision. Gaia data revealed new sub-structures in the main sequence, in the giant branch, and the white dwarf sequence thus never seen before in the HRD. Moreover, these data allow it to reconstruct the history of our galaxy resulting from different merging processes happened in the past. Furthermore, with Gaia it was possible to definitively confirm the bar of the galactic bulge first discovered by the Hipparcos mission, and to measure the so-called secular aberration using quasars (i.e., very far bright objects). Secular aberration is analogous with the annual aberration, but with the Sun moving around the galactic centre during a "platonic" year. The forthcoming releases of the Gaia catalogue promise even more spectacular results revolutionising our view of the Milky Way.

The content of this issue of SPATIUM is based on a talk given by Dr Michael Biermann from the Astronomisches Rechen-Institut (ARI) des Zentrums für Astronomie der Universität Heidelberg, Germany, on April 24, 2024, organized by the Pro ISSI association at the International Space Science Institute (ISSI) in Bern, Switzerland. Dr Biermann is head of the Gaia, JASMINE, and Spacecraft Digital Twins missions at ARI and member of the Gaia Data Processing and Analysis Consortium (DPAC), as well as head of the European Astrometry Group of DPAC.

Andreas Verdun

[1] Altena, W. F. van (2013): Astrometry for Astrophysics. Methods, Models, and Applications. Cambridge, University Press. **[2]** Amelio, G. F. / Tompsett, M. F. / Smith, G. E. (1970): Experimental Verification of the Charge Coupled Device Concept. The Bell system technical journal, 49:593–600. **[3]** Binney, J. / Tremaine, S. (1987): Galactic Dynamics. Princeton, University Press. **[4]** Eichhorn, H. (1974): Astronomy of Star Positions. A critical investigation of star catalogues, the methods of their construction, and their purpose. New York, Frederick Ungar. **[5]** Fricke. W. / Kopff, A. (1963): Fourth Fundamental Catalogue (FK4). Veröffentlichungen des Astronomischen Rechen-Instituts Heidelberg, No. 10. Karlsruhe, G. Braun. **[6]** Grijs, R. de (2011): An Introduction to Distance Measurement in Astronomy. Chichester, Wiley. **[7]** Jin, W. / Platais, I. / Perryman, M. A. C. (2008): A Giant Step – From Milli- to Micro-Arcsecond Astrometry. IAU Symposium 248. Cambridge, University Press. **[8]** Kopal, Z. (1968): Telescopes in Space. London, Faber & Faber. **[9]** Kovalevsky, J. / Mueller, I. I. / Kolaczek, B. (1989): Reference Frames in Astronomy and Geophysics. Dordrecht, Kluwer. **[10]** Kovalevsky, J. (1995): Modern Astrometry. Berlin / Heidelberg, Springer Verlag. **[11]** Kovalevsky, J. / Seidelmann, P. K. (2004): Fundamentals of Astrometry. Cambridge, University Press. **[12]** Kurth, R. (1967): Introduction to Stellar Statistics. Oxford, Pergamon Press. **[13]** Mihalas, D. / Binney, J. (1981): Galactic Astronomy – Structure and Kinematics. Second edition. New York, W. H. Freeman. **[14]** Morrison, L. V. / Gilmore, G. F. (1994): Galactic and Solar System Optical Astrometry. Cambridge, University Press. **[15]** Newell, H. / Smith, H. J. / Roman, N. G. / Mueller, G. E. (1967): Astronomy in Space. NASA SP-127. Washington, NASA. **[16]** Philip, A. G. D. / Upgren, A. R. (1989): Star Catalogues – A Centennial Tribute to A. N. Vyssotsky. Schenectady, L. Davis Press. **[17]** Trumpler, R. J. / Weaver, H. F. (1953): Statistical Astronomy. Berkeley / Los Angeles, University of California Press. **[18]** Walter, H. G. (2000): Astrometry of Fundamental Catalogues. The Evolution from Optical to Radio Reference Frames. Berlin / Heidelberg, Springer Verlag. **[19]** Webb, S. (1999): Measuring the Universe. The Cosmological Distance Ladder. Chichester, Springer Praxis.

Gaia

The astrometric space observatory that is revolutionising our view of the Milky Way

Astronomy is experiencing a golden age in this century. Never before has there been such a wealth of excellent observational data from a wide variety of instruments—both on the ground and in space—and recorded in a wide range of frequencies from long-wave radio radiation to short-wave gamma rays. However, practically all astronomical catalogues suffer from a considerable deficit: they either do not contain the distances of their sources, or these distances are quite inaccurate.

Why are distances so important? Without knowing the distance to a star or other astrophysical object, we can neither determine its true size nor the true amount of energy emitted per second. We only see the (distance-dependent) apparent diameter in the sky and the (distance-dependent) apparent brightness. Due to this fact, we cannot decide whether we are observing a particularly bright object at a large distance or a nearby faint object. Without knowing the true size of an object and the true amount of energy or radiation it produces, an understanding of its nature and physics is largely impossible (Bastian, 2013).

Recognising this, the European Space Agency ESA has taken on the global lead in the creation of space-based astrometric data catalogues, which for all observed sources provide not only positions, proper motions and other astronomical and astrophysical parameters, but also the distance to the source with extremely high accuracy.

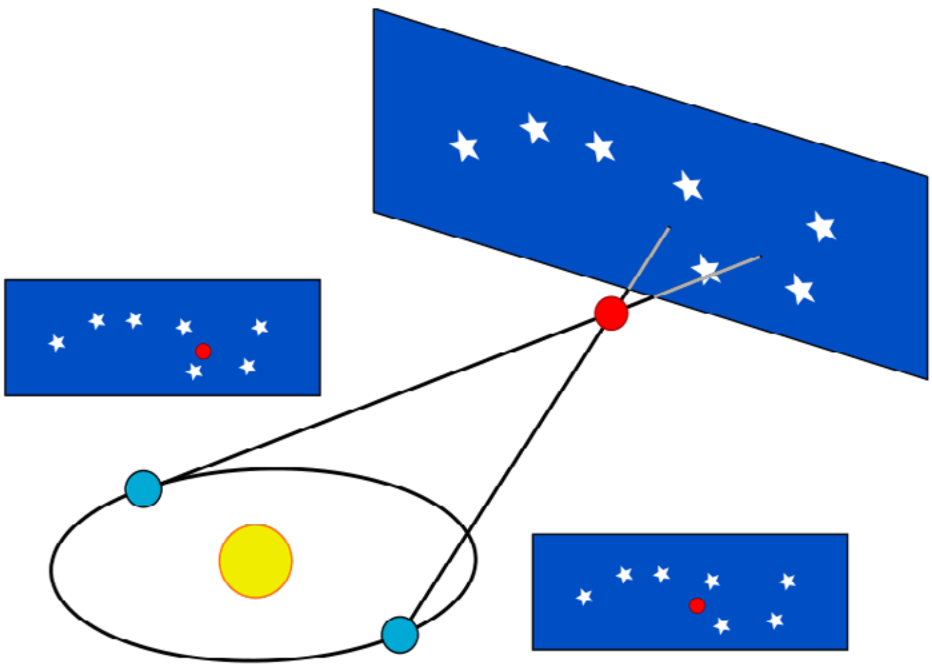

__Figure 1.__ Over the course of a year, a nearby star is seen from the Earth orbiting the sun at different angles against the background of more distant stars. The nearby star therefore moves apparently in an annual ellipsis w.r.t. the background stars, which corresponds to the projection of the Earth's orbit onto the sky. Credits: Wikimedia Commons

Unprejudiced distance measurements

Over the centuries, astronomers have developed a number of methods to determine distances in the universe. Almost all of them have to make assumptions about the object whose distance they want to determine. For example, certain supernovae (of Type Ia) can be used to determine the distances of galaxies which host these supernovae, by assuming that they all explode at the same intrinsic mass and thus shine with the same brightness. Apart from determining distances using radar echoes, which can only be used in, but not outside the solar system, there is only one unprejudiced method for determining distances that does not have to make any assumptions about the object it wants to measure: the trigonometric parallax method.

This trigonometric method makes use of the fact that a star—or any other celestial object—is seen over the course of a year in Earth's orbit from different angles against the background of even more distant stars (**Figure 1**). Over the course of a year, this creates a tiny perspective pendulum motion of the stars, which reflects the projection of the Earth's orbit onto the sky. The further away a star is, the smaller the magnitude of this apparent movement. This is precisely how we humans can estimate distances, because our two slightly offset eyes see close objects at a slightly different angle relative to the more distant background, so the object in front of the background jumps back and forth slightly when you look at it first with one eye and then with the other. The magnitude of this apparent elliptical motion corresponds to half the angular diameter of the Earth's orbit as seen from the star. For sufficiently close stars with precisely known parallax ϖ, this is inversely proportional to the distance r:

$$r\ [\mathrm{pc}]=1/(\varpi\ [\mathrm{arcsec}])$$

if the distance is given in parsecs (about 3.26 light years) and the parallax in arcseconds (a full circle has 360 degrees, and each degree has 3600 arcseconds).

Stellar parallaxes are extremely tiny: one milli-arcsecond is the angular extent of the size of a man on the moon as seen from Earth. The typical parallax of a star in our Milky Way is only 0.1 milli-arcseconds. To determine this to at least 20% accuracy, one must achieve an accuracy of 20 micro-arcseconds. This value is the target precision set for the Gaia mission. Similarly, we would like to know the proper motions measured by Gaia with an uncertainty of a few dozen micro-arcseconds per year.

Figure 2. *Gaia, an artist's impression. Credits: ESA/ATG medialab; background image: ESO/S. Brunier*

ESA's Gaia-Mission

The Milky Way, our home galaxy, is a system of gas, dust, dark matter and around 200 billion stars, many of them have planetary systems. We have known for a long time that it is a galaxy with spiral arms in a stellar disk around a central bulge, and even with an inner bar (Dehnen, 1999). But we on Earth moving around the center of the Milky Way together with the sun find it very difficult to get an accurate, detailed overall view of its structure and composition. One reason for this is that dust clouds within the Milky Way prevent us from seeing the stars behind them, or at least make it difficult, but the main reason is that we have not yet been able to determine the exact distances between us and the stars and are therefore unable to obtain a three-dimensional image. However, a three-dimensional image alone is not enough to get a correct picture of our Milky Way. To really understand it, we also need to know the motions of the stars, because the galaxy is a dynamic system whose history of formation and development we also want to understand. For a huge sample of stars, these high-precision positions and motions can only be determined in space with astrometric satellite missions, unaffected by refraction and scintillation caused by the Earth's atmosphere as well as by mechanical and thermal bending of the instruments.

The history of the successful Gaia space mission (**Figure 2**) goes back to the nineties of the last century, when the Hipparcos mission (Perryman et al., 1997) was flown. The Hipparcos space vehicle observed 120,000 sources in the optical wavelength regime and very precisely determined their positions, proper motions and parallaxes. More than 3,000 scientific publications are based on the results of this astrometric space mission.

The success of the Hipparcos mission let people in 1993 plan an even more ambitious space mission that aimed at providing 50 times more precise positions, proper motions and parallaxes, for 10,000 times more stars! In addition, photometric measurements for all these stars provide their brightness (in the Gaia G-band: 330–1050 nm), their colour in two wavelength bands (blue photometer: 330–680 nm, red photometer: 330–1050 nm), plus spectroscopy (847–874 nm) for about 100 million of its brightest celestial objects to derive their chemical composition and the radial component of their velocities. Based on all these observational data, a dedicated processing of more complex objects like non-single stars or extended objects (e.g. galaxies) is performed, a huge variety of variable sources is identified and characterized, and astrophysical parameters like the surface temperature, chemical composition, and gravity are derived.

The European Space Agency ESA selected this Gaia mission in 2000 as the new Cornerstone mission. Airbus Defense and Space took the industrial lead of the manufacture and assembly of the Gaia satellite and its instruments. On December 2013, Gaia was successfully launched from French-Guiana (**Figure 3**).

More than 1000 engineers and technicians as well as 100 ESA employees have built the Gaia satellite, and a small subgroup of these has supported the commissioning phase from December 2013 to July 2014, when the Gaia spacecraft and its instruments were thoroughly tested.

Figure 3. Lift-off of the Russian Sojus-ST rocket with the Gaia satellite on board from Kourou in French-Guiana in December 2013. Credits: ESA - S. Corvaja

Originally designed for 5 to 6 years, Gaia has now been observing continuously almost every day for more than 10 years and is expected to continue doing so until mid-January 2025.

Gaia operates from a 200,000 km diameter Lissajous orbit around the Lagrange point L2 of the Earth-Sun system. This L2 lies 1.5 million kilometers behind the Earth as seen from the Sun, and is moving together with the Earth around the Sun. The Lissajous orbit is a quasi-periodic trajectory around L2, which lies mainly in a plane perpendicular to the Earth-satellite line. Over the course of a year, Gaia thus orbits the Sun along with the Earth.

Gaia observes with two mirror telescopes of the same type, simultaneously targetting two fields of view 106.5 degrees (the basic angle) apart in the sky (**Figure 4**). Using 10 different mirrors (**Figure 5**), both fields of view are imaged on the same focal plane. During science operations, Gaia rotates slowly every 6 hours about an axis perpendicular to the two lines of sight, and its axis of rotation precesses over the course of 63 days, so that the entire sky is scanned repeatedly over time.

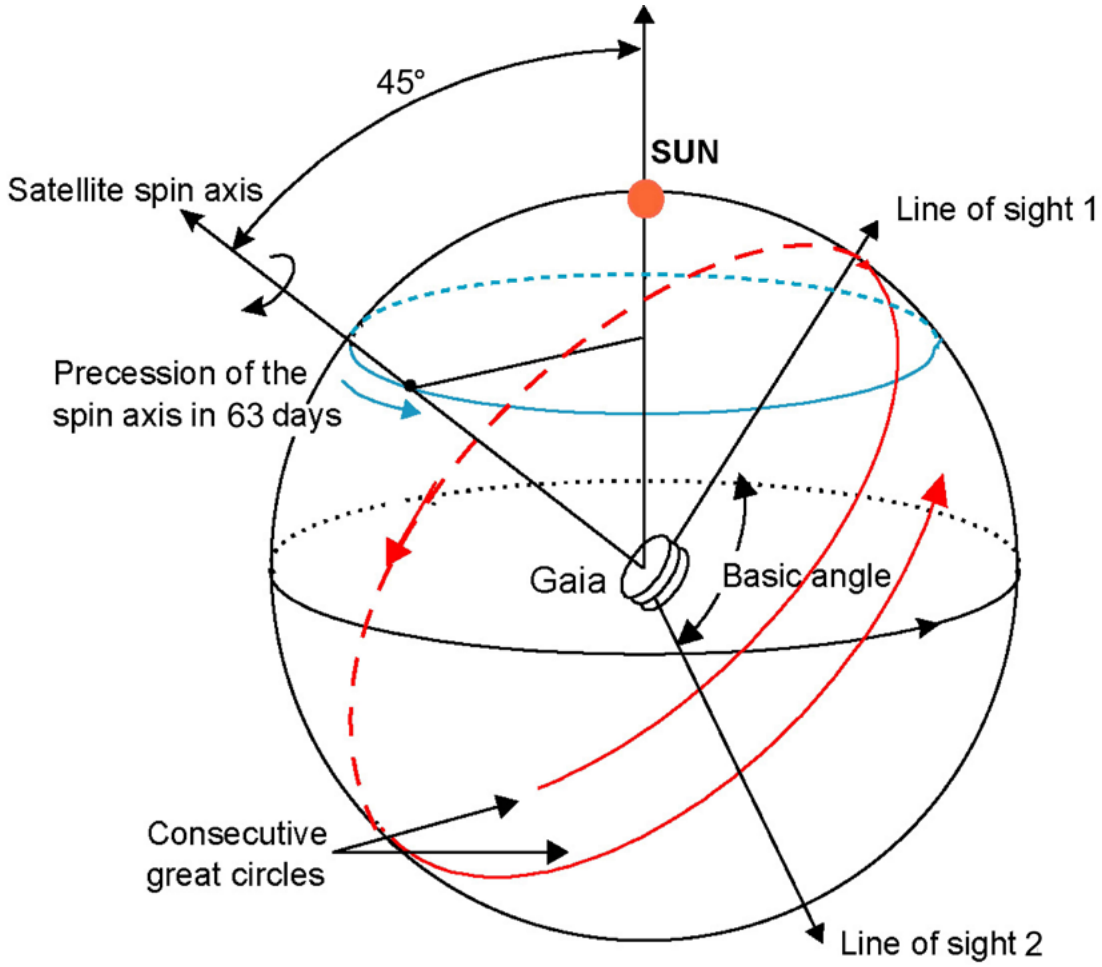

Figure 4. *Gaia continuously spins around its axis, with a constant speed of 60 arcsec/s. As a result, over a period of 6 hours, the two astrometric fields of view scan across all objects located along the great circle ‚perpendicular' to the spin axis. Gaia's spin axis does not point to a fixed direction in space (or in the sky) but is carefully controlled so as to precess slowly in the sky. As a result, the great circle that is mapped out by the two fields of view every 6 hours changes slowly with time, allowing repeated full sky coverage over the mission lifetime. Credits: ESA*

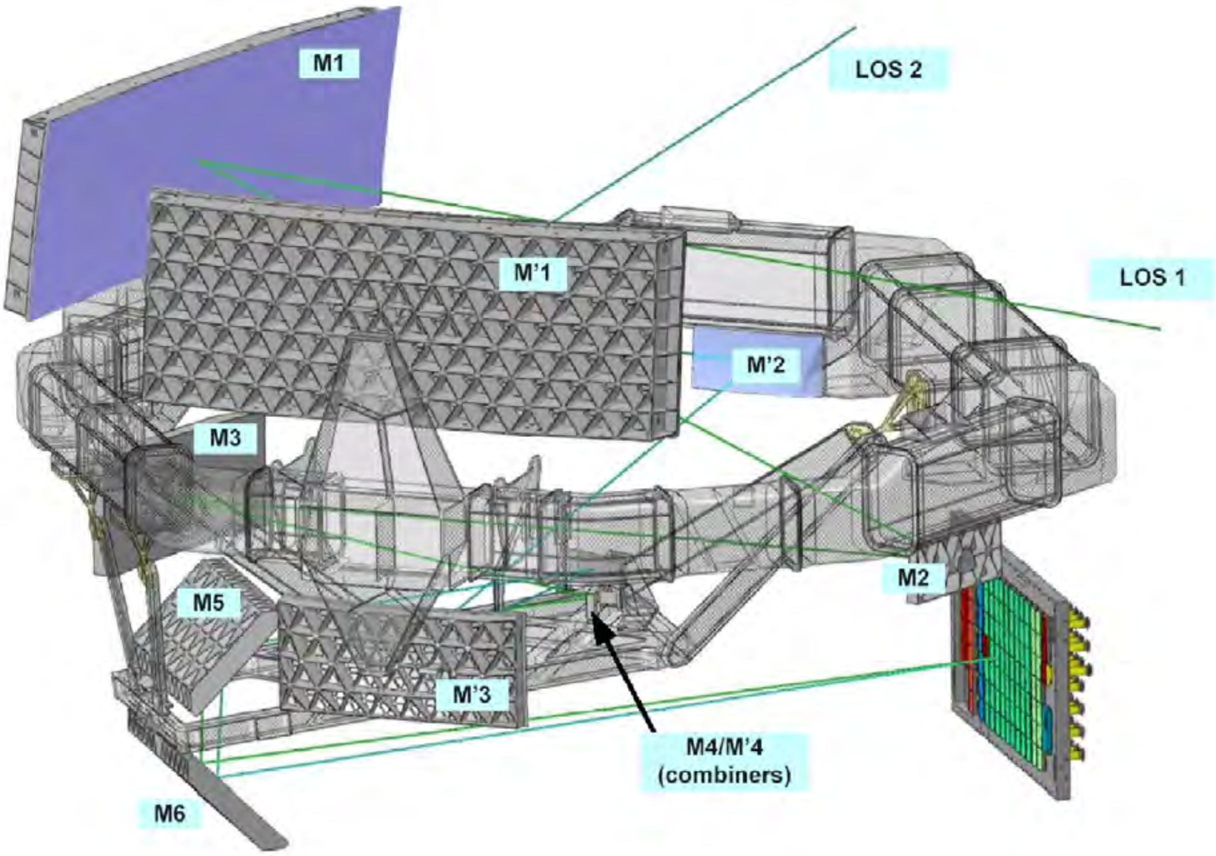

Figure 5. *The optical path of both telescopes is composed of six reflectors (M1-M6), two of which are common (M5-M6). The entrance pupil of each telescope is 1.45 x 0.5 m² and the focal length is 35 m. The payload module features a common focal plane shared by both telescopes. Credits: ESA*

Gaia's instruments

The Gaia satellite is equipped with three different instruments and 106 CCDs which are all arranged on the same focal plane (**Figures 6 and 7**). CCDs are an acronym for "Charge Coupled Device", i.e., electronic light detectors composed of picture elements (called "pixels") each of 10x30 microns in size that produce photoelectrons (charges) caused by the photons accumulated during a 4.4-second exposure time. The three Gaia instruments are (Gaia Collaboration, 2016a)

- **the main astrometric field (AF)**, composed of 62 CCDs, provides two-dimensional angular position measurements in the sky (after the Gaia data reduction, see further below) of all objects down to 20.7th magnitude, which corresponds to the brightness of a candle in 30.000 km distance;
- **the blue and red photometers (BP and RP)**, composed of 14 CCDs, provide low-resolution, spectro-photometric measurements for all objects down to 20.7th magnitude over the wavelength ranges 330–680 nm and 640–1050 nm, respectively;
- **the radial-velocity spectrometer (RVS)**, composed of 12 CCDs, collects high-resolution spectra of all objects brighter than 17th magnitude.

With one billion pixels, Gaia contains by far the largest CCD camera that has ever flown in space. Due to the rotation of Gaia, stars enter on the left side of the array and move to the right (**Figure 6**). At the same time, the charges generated by the

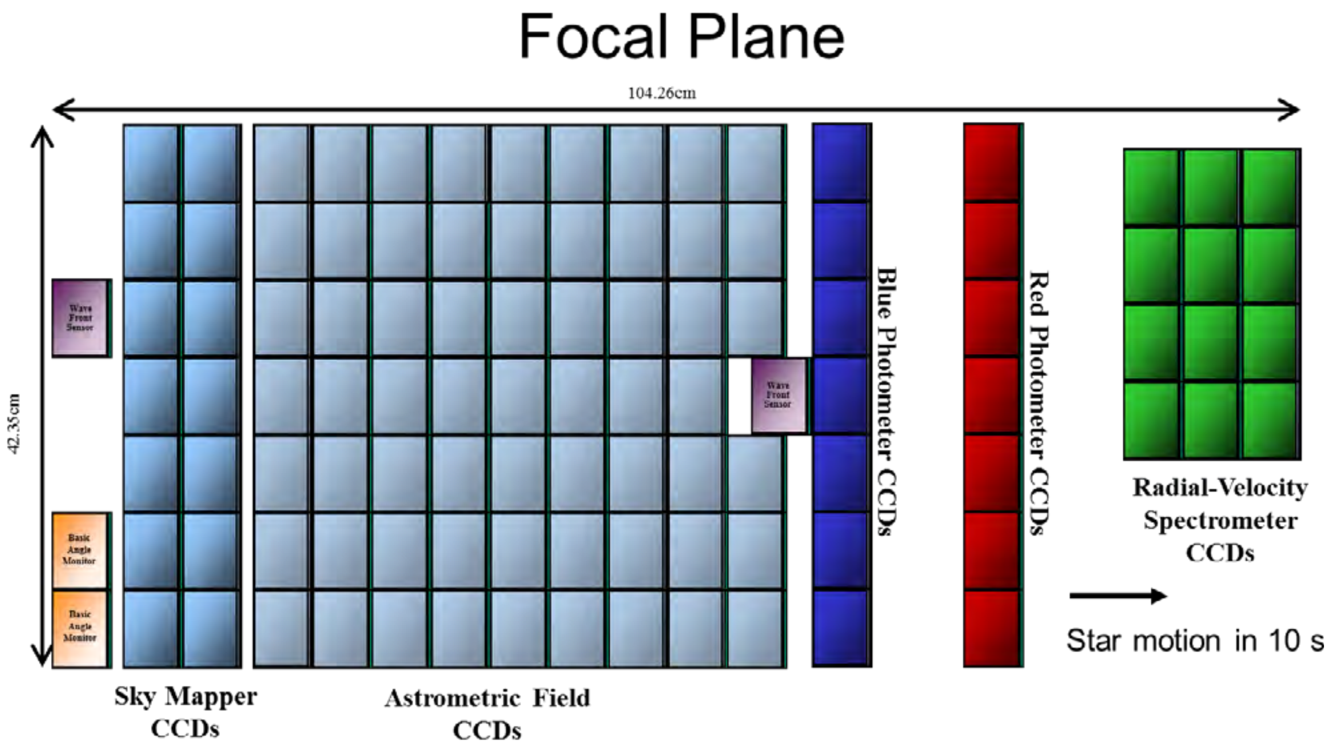

***Figure 6.** The Gaia focal-plane assembly is the largest ever developed for a space application, with 106 CCDs, a total of almost 1,000 million pixels, and a physical dimension of 1.0 m × 0.4 m. Image Credit: ESA. Acknowledgement: Alex Short.*

incoming light on the CCDs are transferred to the right in the direction of the readout register at the same speed as the stars move across the focal plane. This ensures that the images are optimally sharp.

First, stars are seen on the Sky Mapper CCDs (gray-blue). Each Sky Mapper CCD column only sees stars from one field of view. In this way it is already roughly clear in which direction this star was seen. The onboard software reads out all pixels for these CCDs and searches for images of stars in the pixel data. The position of the same stars in the data streams of the CCDs of the astrometric field (gray) is then predicted based on their Sky Mapper position and the knowledge of the exact rotation rate of the satellite. Small pixel areas (called "windows") are cut out around these predicted star positions, and only these are read out and sent to the ground. This is necessary to keep the telemetry budget (i.e. the limited amount of data that can be sent to Earth) at a manageable level.

Prisms and color filters are mounted above the photometric CCDs (blue and red) that follow directly after the astrometric field. The stellar images are pulled apart into short spectra in the direction of movement, which enables brightness and color measurements. Like in the astrometric field, the positions of the spectra in the data stream are predicted and cut out.

A grating spectrograph is located in front of the spectroscopic CCDs (green), which is used to generate relatively high-resolution spectra in the near infrared. These spectra are 1000 pixels long, and their position is again predicted, cut out and sent to Earth.

The four remaining CCDs are used as two detectors each for monitoring the stability of the basic angle (the angle between the two telescopes, orange) and for focusing the telescopes (violet).

Gaia's CCDs are read out in the so-called time-delayed Integration (TDI) mode. This means that the photoelectron charges are shifted in the direction of the CCD's readout register with the same speed as the image of a star moves across the focal plane due to the satellite's rotation. The charges are shifted every millisecond, resulting in a continuous

Figure 7. The complete Gaia CCD array (flight model) - This photo, taken at the Astrium France facility in Toulouse, shows the complete set of 106 CCDs that make up Gaia's focal plane. From left to right: 3 strips for the Radial Velocity Spectrometer, 1 strip for the Red Photometer, 1 strip for the Blue Photometer, 9 strips for the Astrometric field (except for the middle CCD of the first, which is a wave front sensor), 2 CCD for the sky mapper, 1 strip with 3 CCDs: two basic angle monitors (top right), and one wave front sensor. Credits: Astrium

band of read-out pixels with a width of 4500 pixels (the CCD height) times $3.15 \cdot 10^{11}$ pixels (10 years of pixel columns, read out every millisecond) for each CCD.

Gaia typically observes 250 stars per second, for which in a fully automated way nine astrometric, two photometric, and for the brightest 5% of all sources also three spectroscopic measurements will be taken.

More than 2.4 trillion astrometric and more than half a trillion photometric measurements have been made since the start of the scientific Gaia mission in July 2014.

Gaia data reduction

The extremely high target precision (for both position and parallax) is a challenging endeavor. It is complicated by the fact, that the actual observations are made in the data space of the CCD pixel readouts. Data space refers to the set of 3.15·1011 times 4500 digitized pixel readouts per CCD for a 10 years mission. For each observed star image in this data space, a centroid, i.e., the center of the star's light distribution, is computed and stored in the form of data-space (pixel) coordinates.

To convert these data-space coordinates into real positions in the sky, the absolute spatial orientation of the 3-meter large satellite in the Solar System must be known to an atomic diameter – and this for every single moment of the mission. With comparable precision we need to know the arrangement of the 106 CCD detectors on the focal plane and that of all ten telescope mirrors mounted on a ring of silicon carbide that is known to have excellent thermal stability (**Figure 5**).

It is completely impossible to determine the geometry of the instruments and mirrors with such precision in the laboratory. In addition, the extreme mechanical loads during the launch, the absence of gravity in space, and the cooling of the satellites by more than 100 °C make such pre-launch knowledge obsolete anyway. The Gaia instruments therefore have to be calibrated in space, and that can only be done with the satellite's own measurements in the sky.

For just the astrometric part of the data reduction, this self-calibration procedure must simultaneously determine 17 billion star parameters and several hundred million calibration and position/orientation parameters of the satellite from more than 2.4 trillion astrometric measurements using a parameter estimation procedure based on the method of least squares adjustment. However, the extremely high target precision of 20 micro-arcseconds (**Figure 8**) can only be reached if the position of the stars in the data space has been determined to significantly better than 1/100 pixel from the pixel data in pre-processing steps, and if all 2.4 trillion individual observations have been assigned to a total of 2.8 billion astronomical objects in a process known as cross-matching. The photometric and spectroscopic data processing and all subsequent tasks are also extremely complex.

In 2005, the Data and Processing Analysis Consortium (DPAC) was set up, comprising about 430 scientists and software developers spread over 136 institutes in 24 different countries and the ESA (**Figure 9**). DPAC takes care of all aspects of the Gaia data reduction, the validation of the catalogue data and the publication of a series of every increasing and improving Gaia catalogues.

The DPAC consortium splits into different Coordination Units (CUs, **Figure 10**), each responsible for a certain aspect of the DPAC processing: CU1 (System Architecture) provides software packages that are used by all other CUs in a centralized place, CU2 (Simulations) generates complex large-scale simulation data to help validating software packages, CU3 (Astrometric Core Processing) provides a first estimate of the data-space location and the magnitude for each observation (Initial Data Treatment), followed by a task called First Look which judges the scientific data quality and the instrument health on a daily basis to early detect potential problems. CU3 also matches all 2.4 trillion observations to 2.8 billion

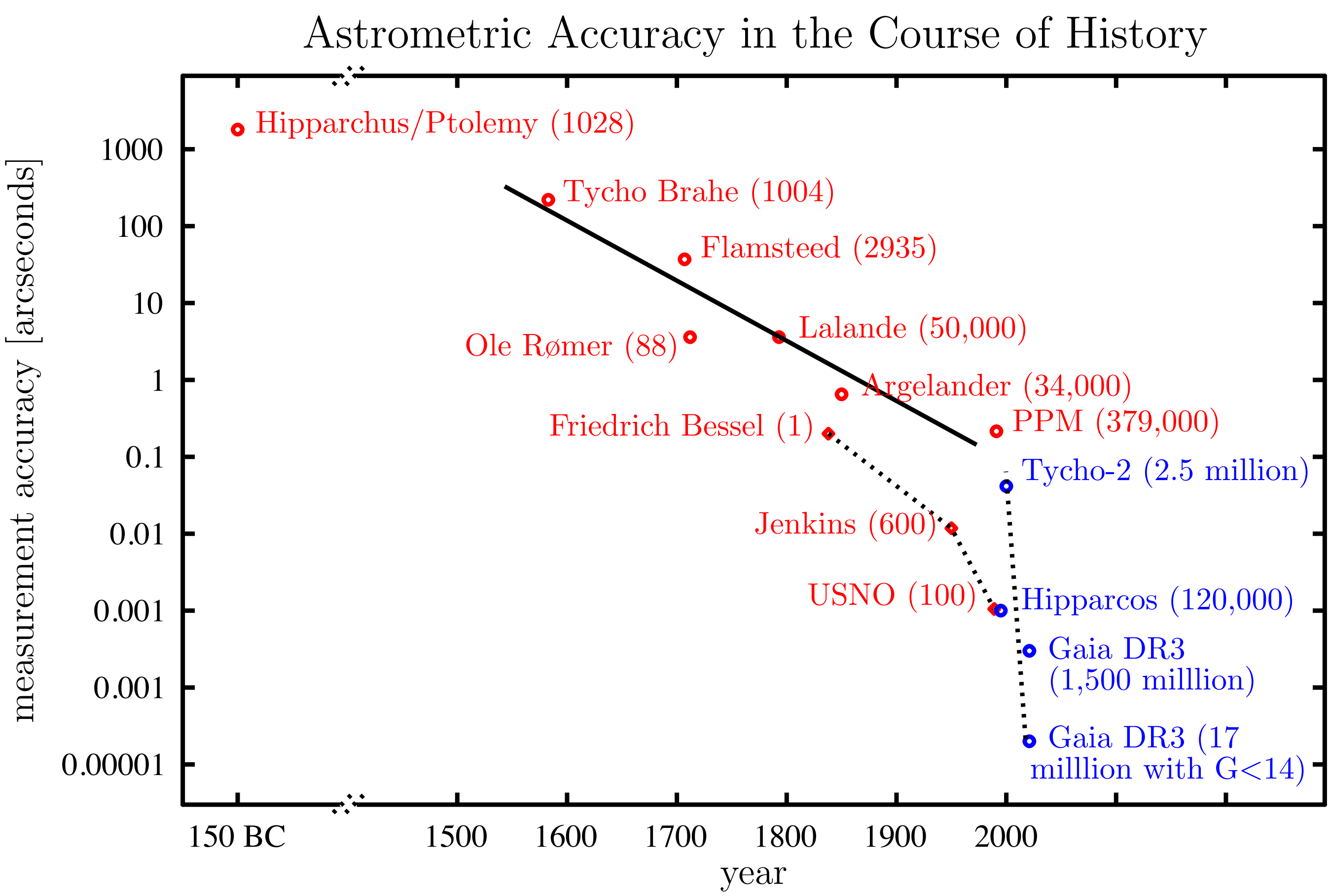

Figure 8. *Position measurements have improved considerably over time. Red circles and the solid line show the measurements of absolute positions (i.e. measurements of large angles up to 180 degrees) from ground, red diamonds and the dashed line show the measurement of relative positions (very small angles between closely neighboring objects in the sky) from ground. Blue circles and the dashed line indicate satellite measurements. The first (scientifically accepted) measurement of a parallax was made by Friedrich Wilhelm Bessel in 1838. Only around 100 more parallaxes could be measured to an accuracy of 20% in the following 60 years, and a further 800 by 1990. Hipparcos suddenly increased this number to 50,000. Credits: E. Høg, M. Biermann*

Figure 9. *A large pan-European team of expert scientists and software developers known as DPAC is responsible for the processing of Gaia's data with the final objective of producing the Gaia Catalogue. Six data processing centers spread over Europe support the data reduction. Credits: ESA*

astronomical objects, produces improved positions and magnitudes and generates the final astrometry for each Gaia catalogue, CU5 (Photometric Processing) and CU6 (Spectroscopic Processing) produce the final photometry and spectroscopy for each catalogue, CU4 (Complex Object Processing) produces astrometric solutions for binary systems and extended objects like galaxies, CU7 (Variability Analysis) identifies and characterises a huge number of different types of variable stars like cepheids or RR Lyrae stars, CU8 (Astrophysical Characterisation) computes among others astrophysical parameters of most sources and finally CU9 (Archive and Catalogue Access) makes all the excellent Gaia data publicly available.

Meanwhile, three Gaia catalogues have been published. The first one, Gaia DR1 (Gaia Collaboration et al., 2016b), was released on September 14, 2016. This first catalogue was more of an appetiser, as it only contained 2 million proper motions and parallaxes. The second DR2 catalogue (Gaia Collaboration et al., 2018), released on April 25, 2018, could already show the enormous potential of the Gaia data and led to thousands of scientific publications. The third Gaia catalogue was published in two steps, first EDR3 (Early Data Release 3, Gaia Collaboration et al., 2020) on December 3, 2020, with "just" the astrometric and photometric data products, and the full DR3 (Gaia Collaboration et al., 2023) on June 13, 2022 with all other data products (**Figure 11**). Each of these catalogues processed more and more data, but also used better and better calibrations and thus achieved significantly better results. Two more catalogues will be published: Gaia DR4 will cover the full nominal 5-year mission plus half a year of the extended mission, and is planned to be released in the first half of 2026. The final catalogue DR5, based on more than ten years of mission data, will become available in 2030.

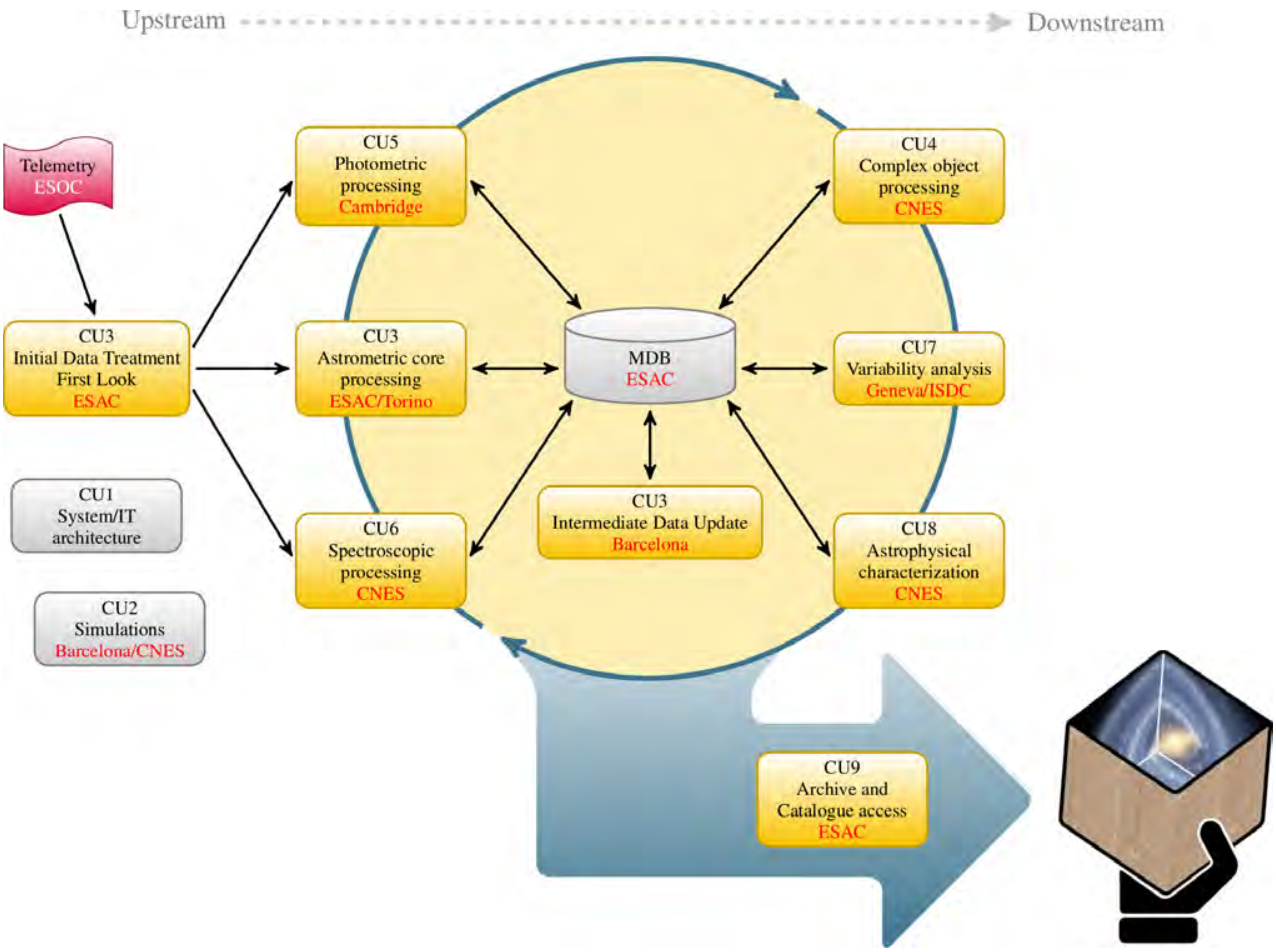

Figure 10. *The consortium is sub-divided into nine smaller, specialist units known as Coordination Units, or CUs, with each unit being assigned a unique set of data processing tasks. The schematic shows the flow of data within DPAC and the roles of the various CUs and DPCs (locations of the latter in red). Credits: ESA, DPAC*

Science with Gaia data

The highly accurate and diverse Gaia data has led to more than 11,000 scientific publications, almost all of them based on the last two interim catalogues Gaia DR2 and DR3. There is practically no field of astronomical research that has not already benefited from Gaia data and will do so to a much greater extent in the future. Just to name a few: Thousands of new asteroids in the solar system have been detected and their orbits determined, the acceleration of the solar system towards the center of the Milky Way could be measured and is in line with theoretical expectation, new insights into stellar astrophysics could be gained, the structure and evolution of the Milky Way has been revealed to much greater detail than ever thought possible, the astronomical distance ladder has been made significantly more accurate, Gaia has improved the International Celestial Reference Frame (ICRF) used by astronomers and geodesists for, e.g., star catalogues and Earth rotation, respectively.

Some of these exciting scientific results will be presented here. The selection is inevitably incomplete and subjectively influenced by the author's interests. But it is also intended to show a little of the wide range of research directions made possible by the excellent Gaia data.

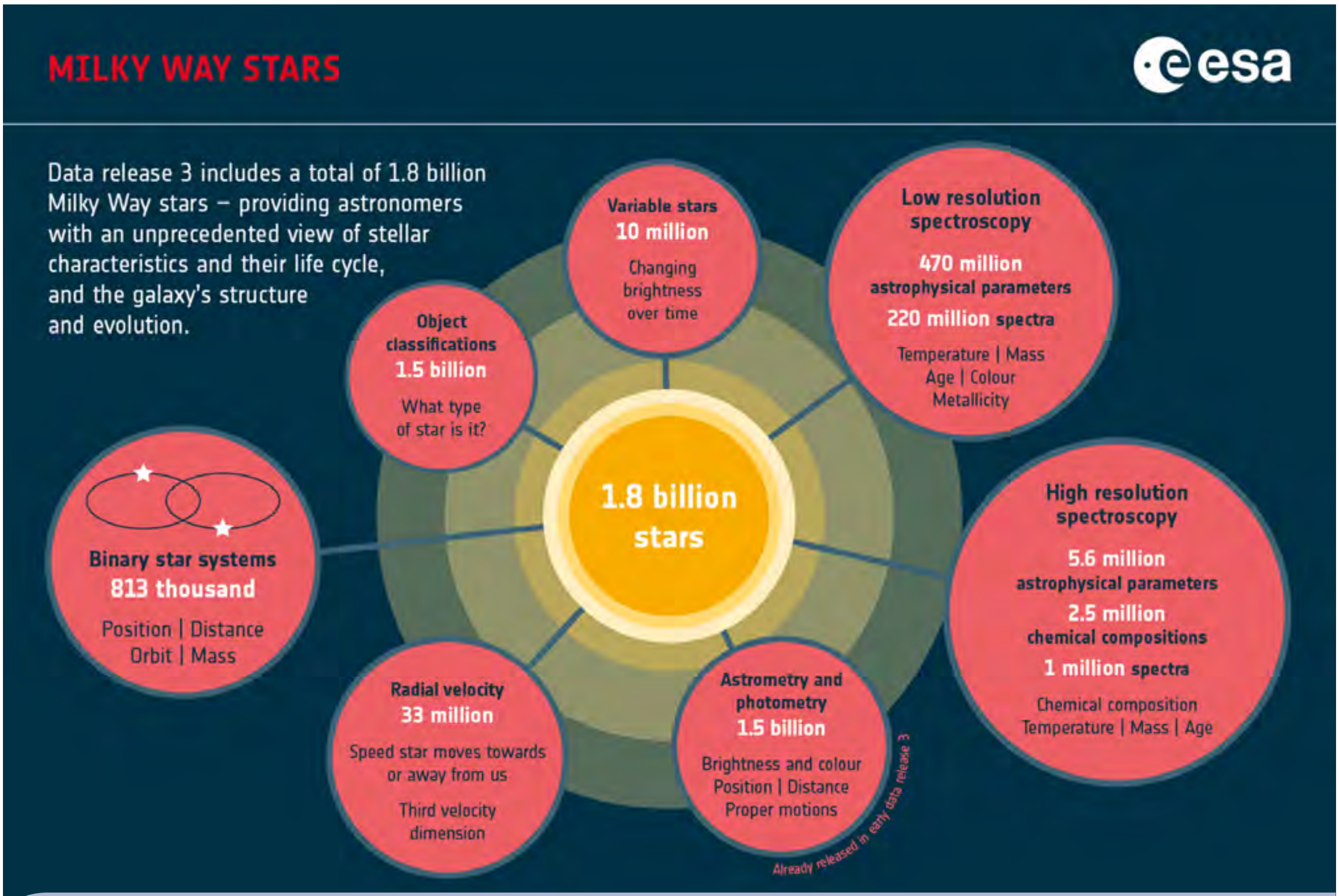

Figure 11. *Data release 3 from ESA's Gaia mission includes a total of 1.8 billion Milky Way stars – providing astronomers with an unprece-dented view of stellar characteristics and their life cycle, and the galaxy's structure and evolution. This infographic shows the various subsets of data that are provided for the stars. Credits: ESA*

Different subgroups of White Dwarfs in the Hertzsprung-Russell diagram

Stars can be arranged graphically according to their colour (or temperature) and absolute magnitude (or luminosity) in a diagram named the Hertzsprung-Russell diagram (HRD). The absolute magnitude of a star is the brightness it would have at a fixed distance of 10 pc (32.6 light years). However, in order to convert measurable apparent into absolute magnitudes, highly accurate distances are required, which have only become available since Gaia parallaxes have been published.

Stars in the solar neighborhood (closer than 100 pc or 326 light years), with 10% accurate parallaxes and good photometry, were selected to create the HRD shown in the top-left panel in **Figure 12**. A corresponding HRD based on 20.000 stars published in the Hipparcos catalogue (top-right panel in **Figure 12**) does not show the fine structures that can be seen in the Gaia counterpart. **Figure 12** clearly shows that most of the stars are arranged in a broad band from the top left (bright blue stars) to the bottom right (faint red stars). An additional, almost parallel band of stars is located further down and to the left, i.e., it contains faint and bluish-white stars. These are white dwarfs.

White dwarfs are the end product of the stellar evolution for stars with moderate masses like our Sun. These stars stay most of their lifetime on the main sequence, the broad major band in the top-left panel in **Figure 12**. Once the nuclear fuel in their cores has been exhausted, they become first red giants (moving above the main sequence) and

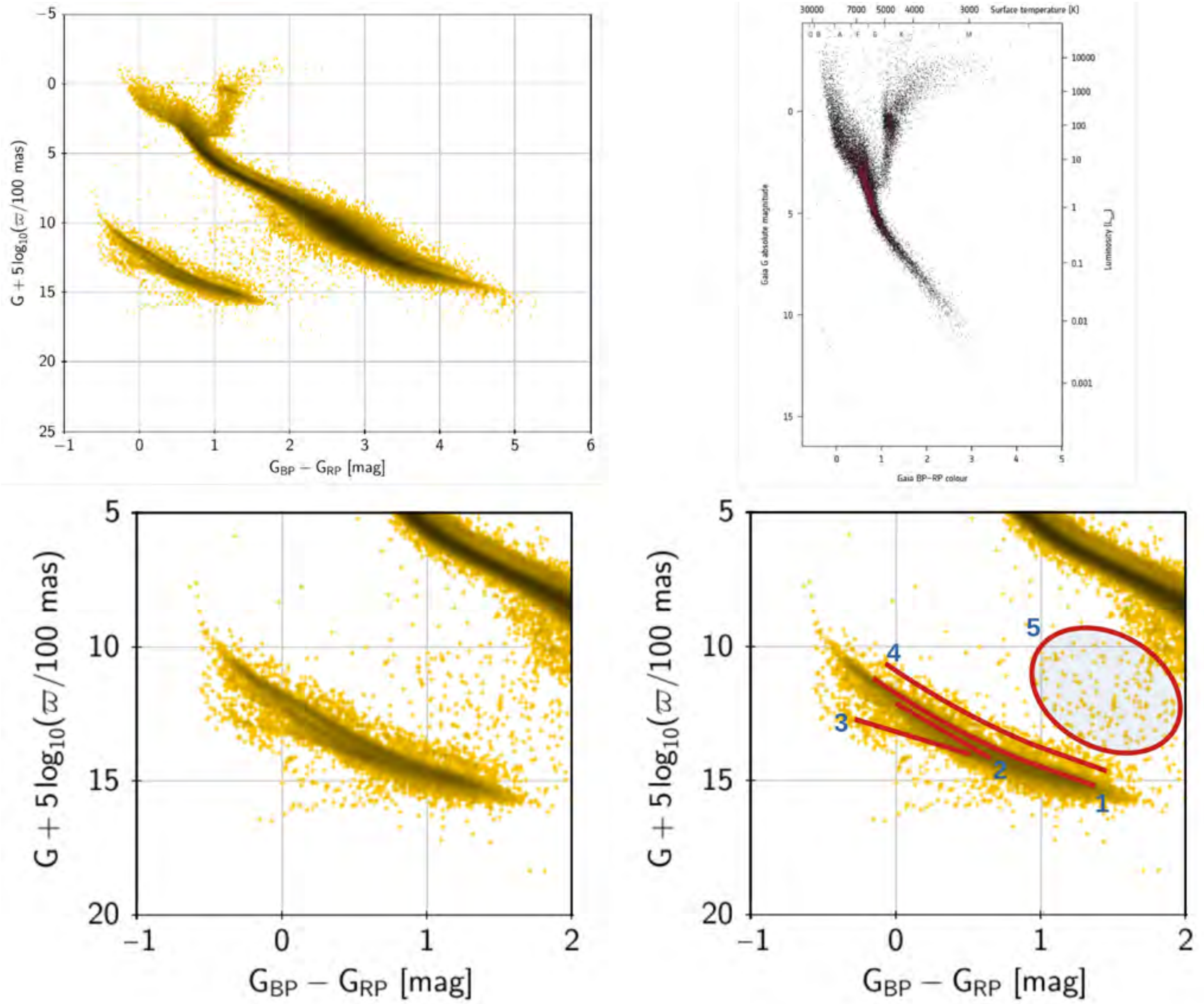

Figure 12. *Top-left panel: Hertzsprung-Russell diagram (HRD) of all stars within 100 pc from the sun and with 10% accurate parallaxes, taken from Gaia DR2 data. Right-top panel: HRD of 20,000 Hipparcos stars. Bottom-left-panel: Zoom-in into the white dwarf sequence of the DR2 HRD. Bottom-right panel: Same as on the left side, but with some white dwarf samples highlighted. For details please refer to the text. Credits: Lindegren et al. (2018), modified by M. Biermann, and ESA/Gaia/DPAC; ESA/Hipparcos; CC BY-SA 3.0 IGO.*

finally lose their outer shells as planetary nebulae while they contract into white dwarfs (moving downwards in the HRD to settle on their own white dwarf sequence.

Before Gaia, about 30,000 white dwarfs were known. With Gaia, this number of white dwarfs could dramatically be increased by a factor of more than 10: more than 300,000 white dwarfs are identified meanwhile in the Gaia DR3 catalogue.

The lower left panel in **Figure 12** is a zoom-in into the complete HRD, focusing on the sequence of white dwarfs. There are some clearly distinguishable accumulations of white dwarfs, marked as five different subgroups on the bottom-right panel of **Figure 12**, which is otherwise identical to its left-hand counterpart:

- There is a dense region of white dwarfs in the HRD marked as red line '1' in the bottom-right panel of **Figure 12**. This region is occupied with white dwarfs whose outer shells essentially contain hydrogen,

- Similarly, region '2' hosts white dwarfs with a helium shell.

- In the course of their stellar evolution, white dwarfs undergo a phase where their cores transform into a crystalline carbon-oxygen core. These white dwarfs can be found in region '3'.

- As normal stars, white dwarfs can be companions in binary systems. If both stars of such a double star system are white dwarfs, and if the system is too far away in order to allow the two stars to be resolved into individual stars, then the combined light of the two white dwarfs will create a signal slightly brighter than the individual white dwarfs and produce a slightly shifted, brighter sequence of white dwarf double stars (region '4').

- Of course, white stars can also be partners of normal main sequence stars in a binary system. Those settle in the HRD somewhere in the roundish region '5', depending on the relative brightnesses of the two components.

High-speed White Dwarfs

A small number of white dwarfs with huge velocities of several 1000 km/s have been identified in the Gaia catalogues. Any stellar source with such extreme velocities is no longer bound to the gravitational potential of the Milky Way and would – on astronomically short timescales – leave our home galaxy. Detecting a number of these high-speed white dwarfs deeply embedded in the galactic stellar disk tells us that these stars have received their enormous space velocities only recently.

Theoreticians have brought up the idea that these high-velocity white dwarfs could have been members of binary systems with two white dwarfs orbiting around each other. The more massive white dwarf of the two companions has collected more and more additional mass over time, until it has become too massive to stay stable as a white dwarf (so-called Chandrasekhar limit). It then has collapsed to a neutron star in a supernova type Ia explosion. Such star explosions completely destroy

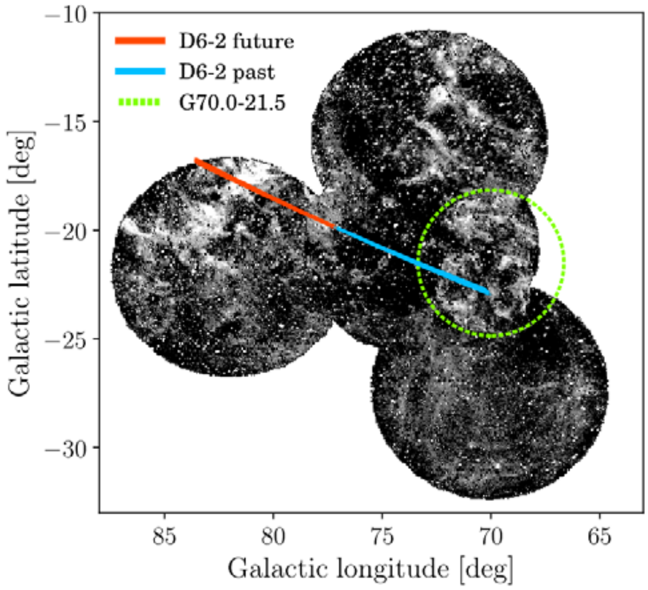

Figure 13. *Orbital solution of the high-velocity white dwarf D6-2 in Shen et al (2018) overlaid on Ha images from the Virginia Tech Spectral Line Survey (VTSS; Dennison et al. 1998). The blue and red trajectories extend 9×10^4 years into D6-2's past and future, respectively. The green circle encompasses the supernova remnant of G70.0–21.5. Credits: Shen et al. (2018)*

the star, so that the less massive companion no longer feels the gravitational attraction of its former partner. The remaining white dwarf would then continue to move through space with the high speed it had on the close orbit when its partner was still present.

If that idea is correct, one could check whether the known 3D velocities from the Gaia catalogue extrapolated back in time would bring high-speed white dwarfs close to a known supernova remnant. Strong evidence in support of this idea has been given in Shen et al. (2018). Not only the position of the high-speed white dwarf named D6-2, extrapolated back in time, meets the position of the supernova remnant G70.0-21.5, but also the time of the supernova explosion nicely fits the time when the back-extrapolated white dwarf position meets the supernova remnant position (within reasonable uncertainties, shown as a green dashed circle in **Figure 13**).

Gaia BH3

Before publishing new Gaia catalogues, a lot of effort is devoted to the validation of the results, in order to ensure the extremely high quality of the Gaia data products. In the course of non-single-star validation runs for the forthcoming fourth Gaia Data Release (to be published in 2026), a stellar black hole (BH) with an extreme mass of 32.7 ± 0.82 solar masses was found only 560 pc (1830 light years) away from the sun.

Of course, we cannot see the black hole itself, but only its companion star whose motion shows an orbital component. This bright star with high proper motion in the constellation Aquilla had

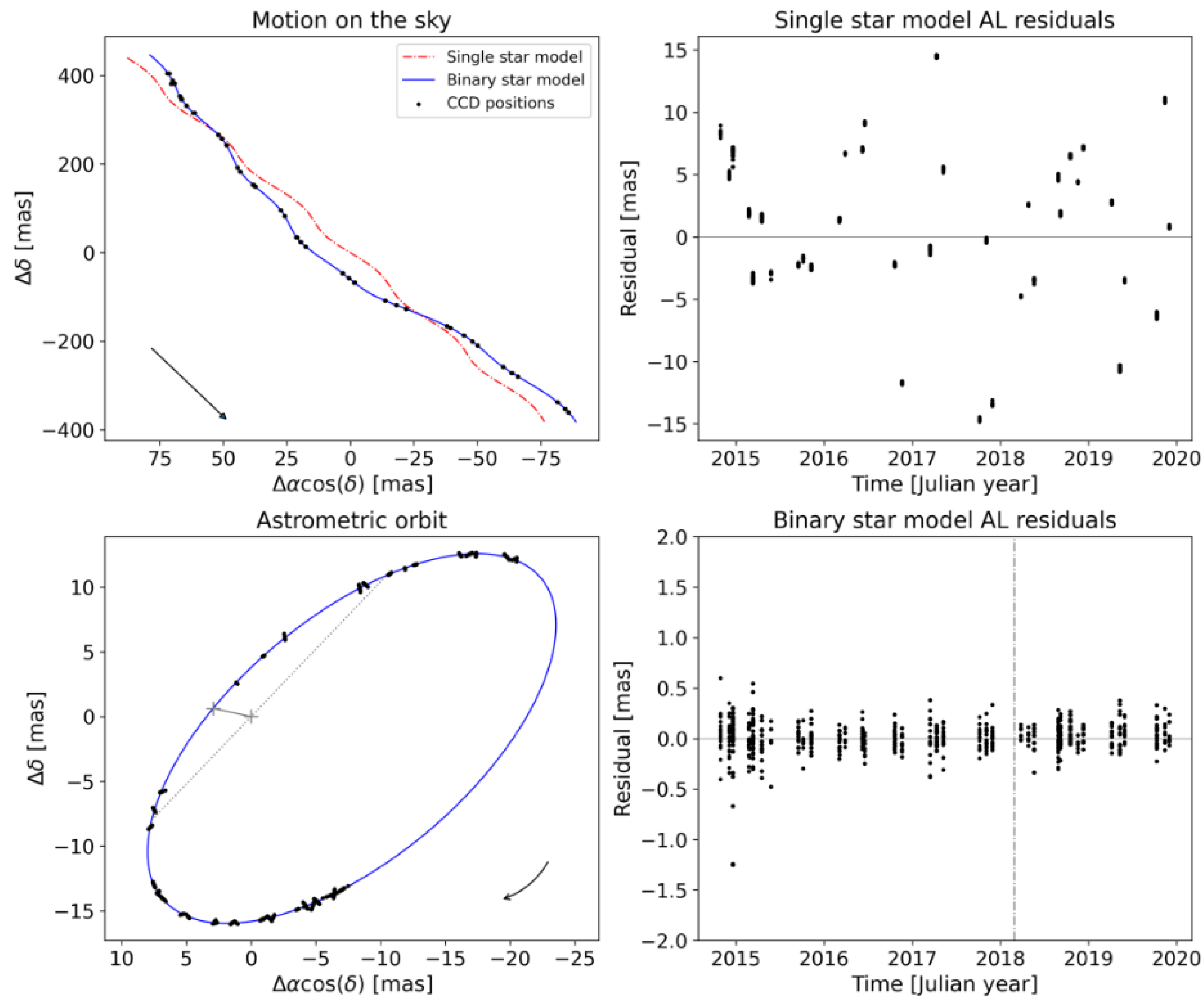

__Figure 14.__ Astrometric data of Gaia BH3. Top-left panel: Motion in the sky of the source, as seen by Gaia (dots), compared with the best fitting single-star solution (red line) and the astrometric-binary solution (black line); the arrow indicates the direction of the proper motion. Bottom-left panel: Derived astrometric orbit of the visible companion, after a subtraction of parallax and proper motion, compared with the astrometric measurements. The arrow indicates the direction of the motion along the orbit. The top-right and bottom-right panels show the residuals of the along-scan (AL) astrometric measurements for, respectively, the single-star solution and the binary-star solution. The vertical dot-dashed line in the bottom-right panel marks the time of the closest approach to the black hole (also marked by the short grey line in the bottom left panel). Credits: Gaia Collaboration et al. (2024)

received a very poor astrometric solution when it was assumed to be a single star. The astrometric residuals (the differences between the observed positions and the positions predicted for the single-star model) were clearly too large (top right plot in **Figure 14**). It was therefore obvious to assume that this star was a partner in a binary system. In this case, all observations perfectly match the derived orbit (after subtraction of the proper motion and the parallax motion, bottom left plot in **Figure 14**), and the astrometric residuals have decreased by a factor of 25 (lower right plot in **Figure 14**), clearly showing that the double-star solution resulting from the least square adjustment is significantly better. With the Gaia RVS radial velocities, a spectroscopic double star solution could be determined which is in excellent agreement with the astrometric solution. However, the partner must have a mass of more than 30 solar masses and be invisible, properties which only a black hole can fulfill.

This black hole BH3 in many ways is a stroke of luck for science and has therefore been published ahead of schedule, more than two years before the planned Gaia DR4 catalogue. First of all, it is more massive than any known stellar black hole in our galaxy, and with a distance of just 560 pc it is very close and thus an optimal candidate for intense follow-up observations with other telescopes. It is true that the gravitational-wave detectors LIGO/Virgo have also detected black holes of similar mass, but only in far distant galaxies. These black holes can never be observed again because they collided with other black holes when they generated the gravitational wave signals. The resulting black hole is no longer noticeable through gravitational waves and cannot be observed in the electromagnetic spectrum due to its small size and great distance.

The formation of massive stellar black holes with more than 30 solar masses is a challenge for stellar evolution models. It is thought to be possible only for low-metallicity stars. In astronomy, all elements heavier than helium are called “metals”, so metal-poor stars are those that built very early in the universe when no heavier elements have already been produced in stars and redistributed to molecular clouds via supernovae or planetary nebulae. Progenitors with an initial mass larger than 30 solar masses are predicted to lose a significant fraction of their mass through strong winds. However, low-metallicity stars show much lower mass losses during their lifetime. It is thus very interesting to find the visual companion of BH3 to be a very metal-poor star. Gaia BH3 is therefore the first observational evidence that high-mass BHs detected by LIGO/Virgo are generated by low-metallicity stars as predicted by stellar evolution models.

Structure and Evolution of the Milky Way

The most noble task of Gaia is to help us better understand our Milky Way, in particular to reveal its spatial structure and physical components, its dynamic structure (i.e. the forces and motions), and to piece together a coherent formation history of our home galaxy. This has already – to quite some extent – been achieved through a large number of exciting scientific publications based on Gaia DR2 and DR3.

Antoja et al. (2018) for instance have analysed phase-space diagrams based on Gaia DR2 data. These are diagrams that show both spatial and

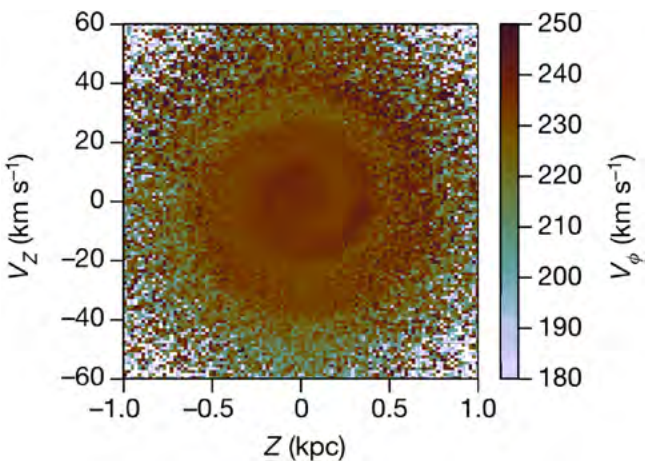

Figure 15. *Phase-space diagram of stars, showing their velocity Vφ (colour-coded) in the galactic stellar disk depending on their velocity V_Z perpendicular to the stellar disk and their altitude Z above or below the midplane of the galactic stellar disk. For the interpretation of this diagram please refer to the text. Credits: T. Antoja et al. (2018)*

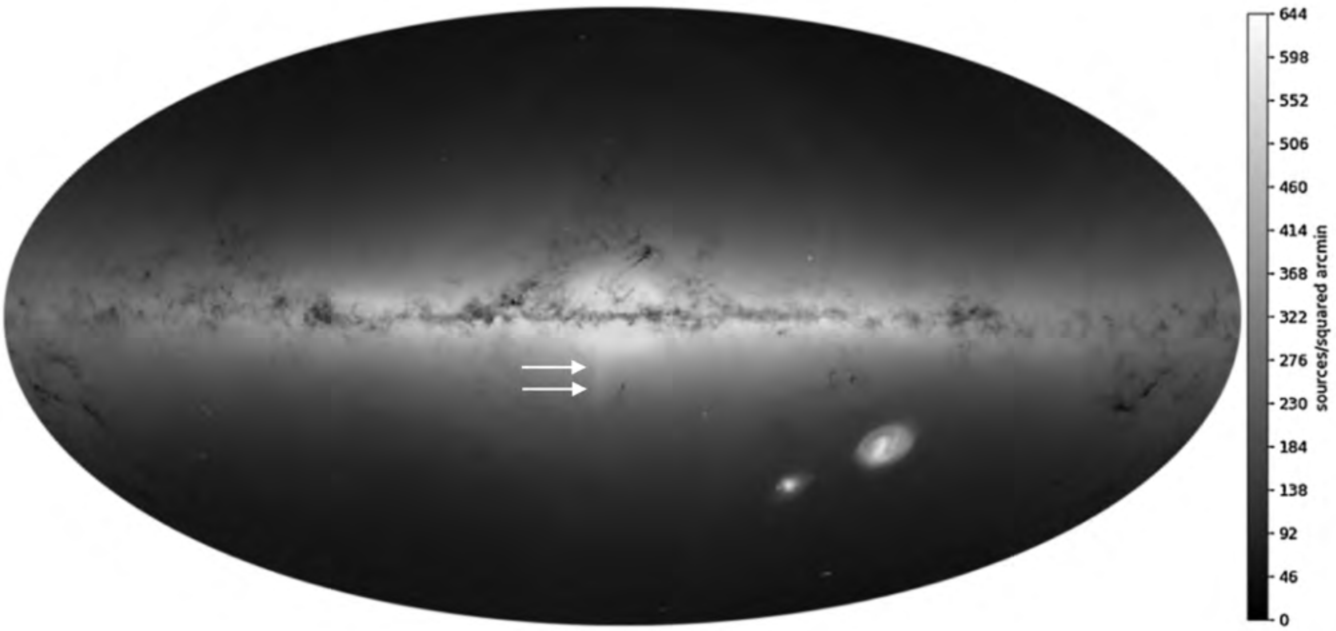

Figure 16. *Sky chart of the Milky Way as seen by Gaia. The Sagittarius dwarf galaxy is visible as a small, vertical whitish streak just below the bright galactic center in the middle of the image. Credits: ESA/Gaia/DPAC, modified by M. Biermann*

velocity information in a single plot. One example is presented in **Figure 15**. This plot shows the (colour-coded) velocity Vϕ of stars in the plane of the galactic stellar disk orbiting the Galactic center as a function of their height Z above or below the midplane of the galactic stellar disk and their velocity VZ perpendicular to that plane. Typical stars in the Milky Way move on more or less circular orbits at a rather fixed radius around the center of the galaxy. In doing so, the stars also move perpendicular to the rotational motion and continuously go up and down, and thus change both the height Z above or below the midplane of the galactic disk and their velocity VZ perpendicular to that plane. It was not expected that coherent structures would appear in the phase-space diagram shown in **Figure 15**, but instead a beautiful spiral emerged. This spiral can be explained by a disturbance in the galactic orbits of the stars 300–900 million years ago, caused by an infall of another galaxy into the Milky Way that probably has penetrated the galactic plane more than once during this still ongoing merging process. It was probably the Sagittarius galaxy that had its latest close approach to the Milky Way about 500 million years ago. The remnant of this dwarf galaxy is still visible on Gaia sky maps (**Figure 16**). But this remnant of an ancient interaction of the Milky Way with another galaxy is not the only one visible in the Gaia data.

The second Gaia catalogue contains both 3D positions and 3D velocities of seven million stars. Of these, 30,000 stars move around the center of the Galaxy on elongated, retrograde orbits, which means that these stars move in the opposite direction to the majority of the stars in our Milky Way (Helmi et al., 2018). In addition, these 30,000 stars have a different chemical composition than most stars in our galaxy. They are interpreted to form the debris from yet another and much bigger galaxy that merged with our Milky Way in its early formation phase about 10 billion years ago. This meanwhile completely assimilated galaxy originally had a mass of approximately 1/10 of that of our current Milky Way, but this corresponds to ¼ of the mass of the Milky Way 10 billion years ago, because the Milky Way has grown substantially over time by merging with other galaxies and ancient stellar structures. Having roughly comparable masses, this merging process must have been a very turbulent one. The former galaxy and today's debris are named „Gaia-Sausage-Enceladus": "Gaia", because this discovery was only possible with excellent Gaia data, "Sausage" because of the shape of the remaining debris in velocity space, and for the "Enceladus" I quote the first author of the discovery paper, Amina Helmi: "According to the legend, Enceladus was buried under Mount Etna, in Sicily, and responsible for local earthquakes. Similarly, the stars of Gaia-Enceladus were deeply buried in the Gaia data, and they have shaken the Milky Way, leading to the formation of its thick disc."

In addition to finding such individual structures and merger events, however, it is and remains a central goal of modern astronomy to create a consistent overall picture of our galaxy's formation history. Of course, long before the Gaia era, there had already been a great deal of research and work on this topic, which had already led to a global picture. This is now to be confirmed, expanded, improved and, if necessary, corrected with the Gaia data.

As a final topic, I will discuss the interplay between the chemical composition and the motion of the stars as a beautiful example of both the power and the complexity of Gaia science applications.

Chandra et al. (2023) have used 10 million red giant stars from the Gaia DR3 catalogue which have good astrometry and the full 6D phase-space information (thus both 3D spatial information and 3D velocities), but also spectral information to derive metallicities of the stars and especially their α-element abundances. α elements are elements like, for example, carbon, oxygen, silicon and iron which are built during nuclear fusion reactions in massive stars or during supernova explosions. This sample of stars serves as an excellent starting point for archaeological studies due to its size, homogeneity, and all-sky coverage (**Figure 17**). As we have astrometric 6D information for all these stars, we also know the orbital properties for their motions around the galactic center. These properties were encoded by Chandra et al. (2023) in the form of an angular momentum ratio η (= L_z/L_c), which is 1 for circular prograde orbits (where the star moves in the same direction as the majority of all stars in the Milky Way), which is -1 for circular retrograde orbits (where the star moves in the opposite direction) and takes values in between for inclined, more chaotic orbits, including polar orbits.

Chandra et al. (2023) have produced a density plot of this ratio η as function of the metallicity, expressed as the ratio [Fe/H] of iron to hydrogen (top plot in **Figure 18**). The Sun has [Fe/H] = 0, and negative values of [Fe/H] indicate stars with less metals (i.e. elements heavier than helium). In this density plot, reddish areas contain many stars, whereas blue ones contain few to almost no stars. The upper diagram in **Figure 18** clearly shows that different subgroups of stars form this density distribution. Even more information can be gained from this top plot by dividing all the stars into two subgroups: one with a large proportion of α elements (high-α, measured as the ratio [α/Fe]) and one with a small content of α elements (low-α) as shown in the two bottom plots in **Figure 18**. These three plots contain a lot of information about the formation history of the Milky Way.

What does the α abundance tell us about the stars in the Milky Way? At the very beginning of the evolution of a galaxy, the first stars are built in gas clouds that consist practically only of hydrogen and helium. However, heavier elements are formed very quickly, especially in supernovae explosions at the end of the lifetime of massive stars, but also in

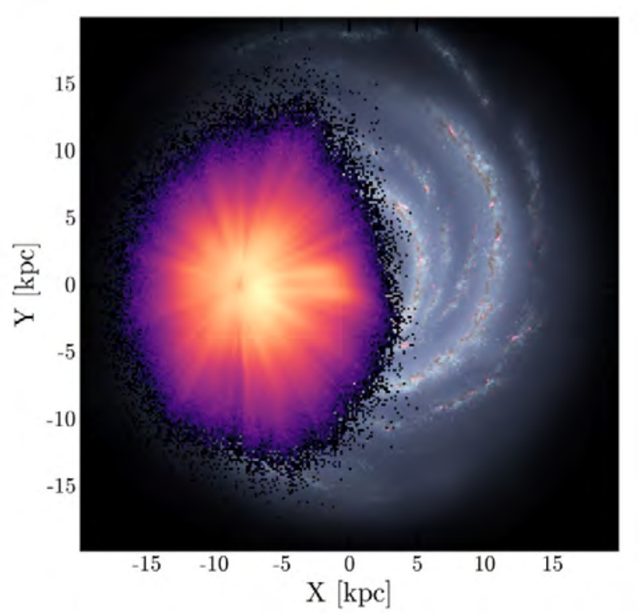

Figure 17. *Spatial distribution of the stars from which the formation history of the Milky Way was determined, superimposed on a schematic image of a spiral galaxy. Credits: Chandra et al. (2023)*

planetary nebulae and massive stellar winds (from the asymptotic giant branch, AGB, in the HRD), so that α elements are quickly enriched in the gas clouds available for the next star generation, while the iron abundance is still low. This leads to high ratios [α/Fe]. Emerging iron remains in the cores of the white dwarfs and neutron stars and does not contribute to [α/Fe]. Much later, when white dwarfs start to explode as supernovae of type Ia and are completely destroyed, the iron will be released and will enrich gas and dust clouds out of which new stars will be born. These stars, which were formed late in the history of a galaxy, thus have low [α/Fe], since the iron content has increased.

What can we learn from the three plots in **Figure 18** about the history and formation of our galaxy? **Figure 19** is the same as the top plot in **Figure 18**, but highlights certain areas giving insight into different formation and evolution stages in the history of the Milky Way.

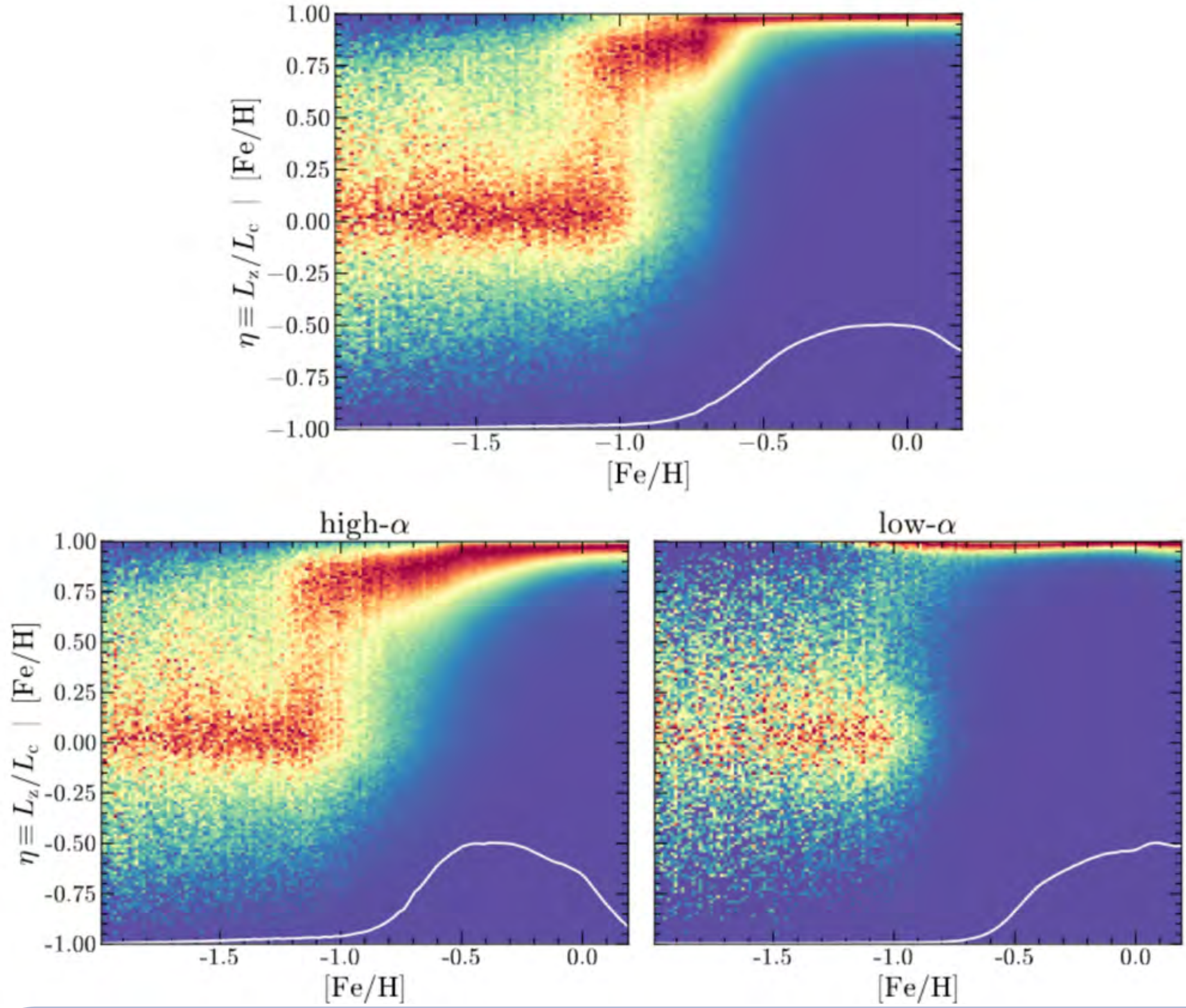

Figure 18. *The three-phase evolution of the Milky Way. The distribution of orbital circularity η is shown as function of metallicity. The top panel shows all stars used in Chandra et al. (2023), whereas the bottom panels are split into high-α and low-α subsamples (see text). Credits: Chandra et al.*

Area ’A’ in **Figure 19** hosts the very old stars that were built in the nascent Milky Way. The stars in this protogalaxy had chaotic and disordered orbits, as the wide spread of η values indicates. The protogalaxy with its still existing old stars show minimal net rotation, but their η distribution is not entirely isotropic. Rix et al. (2023) have shown that the central bulge of the Milky Way indeed hosts an ancient, metal-poor, centrally concentrated stellar population built by the few most massive progenitor components that formed the protogalaxy. The protogalaxy was constantly “bombarded” by mergers. The bombardment caused a first disk to appear, as a consequence of dissipative gas collapse in dark matter halos and the conservation of angular momentum. Area ‘A’ is not centered on zero, which means that the protogalaxy soon had formed such a disk component. The still existing stars of the former protogalaxy are in parts also those of past mergers like the Gaia-Sausage-Enceladus dwarf galaxy and can be found on eccentric orbits. This subsample of stars is clearly visible from the kinematics of the stars and their chemical composition, as discussed above. But if area ‘A’ represents the stars of the nascent, chaotic protogalaxy, why do these stars show high α abundances, as the bottom plots in **Figure 18** clearly shows? Why has this star sample not turned into a low-α bulge as discussed above?

The reason for this is that the iron-enriched gas and dust clouds have been ripped of from the protogalaxy during a massive merger event, so that no iron-enriched stars could form there. This is visible in area ‘B’ in **Figure 19**, which highlights a dramatic phase transition and the emergence of a rotation-dominated disk component (η gets closer and closer to 1, representing circular orbits for the majority of the stars and therefore the stellar disk of the Milky Way). This transition is almost exclusively traced by high-α stars, thus the older galactic stars. Their spatial distribution is getting more and more disk-dominated with time (area ‘C’ in **Figure 19**). This phase transition represents the birth of the Milky Way’s disk over cosmic time, from the turbulent protogalaxy to an increasingly ordered disk. As metallicity (and time) increases, the range of the orientation of orbits spanned by the high-α disk narrows, as stars move on increasingly circular orbits. This gradual development towards a more and more disk-like structure is notably smooth and continuous all the way up to solar metallicity (see lower-left plot in **Figure 18**).

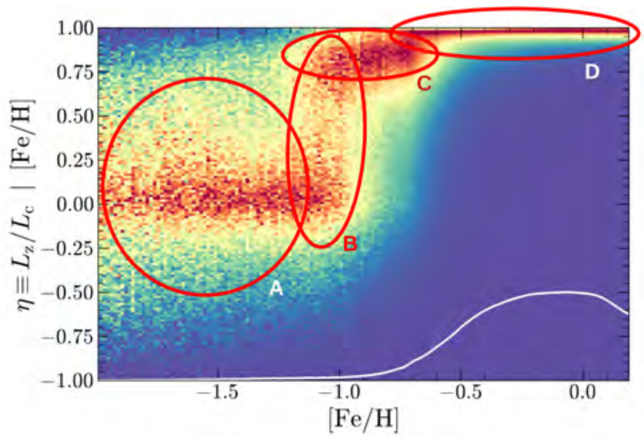

Figure 19. *Zoom-in into the top plot of Figure 18, with important areas highlighted and discussed in the text. Credits: Chandra et al. (2023), modified by M. Biermann*

Between the chaotic protogalaxy (area ‘A’) and the thick disk (area ‘C’), there is a swath of stars at intermediate orbits between the two populations (in the middle of area ‘B’). The most plausible origin for those stars is that they were born in the early Milky Way disk and subsequently kicked up onto isotropic and eccentric orbits by a major merger, presumably the Gaia-Sausage-Enceladus. The thickness of this disk is not only due to the merger disturbing and changing individual orbits of stars but also due to a rotation of the whole disk which has reoriented itself after the merger event.

This reorientation of the disk did not only affect the stars but also the gas of both the Milky Way and the merging galaxy. From this gas, new stars were born. With time, the gas reservoir was enriched with iron, and increasingly more stars were born from this iron-enriched material leading to a high-metallicity but low-α sample of stars on mainly circular orbits (area ‘D’ in **Figure 19**). These stars on very circular orbits are especially visible in the bottom right low-α plot in **Figure 18**. All these stars have been formed in the stellar disk of the Milky Way as we see it today, and they all have near-circular orbits over the full metallicity range.

Is there additional support for this coherent picture of the structure and evolution of the Milky Way? A large amount of complex galaxy evolution simulations have been performed by several groups. The results of these simulations have been compared by Chandra et at. (2023) to the results based on Gaia data. Both nicely match, when simulations are used in which a galaxy has a rapid growth of the early disk component and an early massive encounter/merger with another galaxy, as in the case of our Milky Way.

Outlook

The amazing scientific results presented here are just a tiny fraction of the gigantic spectrum of scientific work that was only made possible by the excellent Gaia data. The full scientific treasure from Gaia data has yet to be raised, and that will take many decades. In addition, the new Gaia catalogues will not only become increasingly accurate, but will also include a variety of new data products that will expand the range of scientific investigations and enable future improved data reductions of the entire Gaia data. In particular, the epoch data (i.e. the individual observations) will make it possible to improve stellar parameters of individual sources that are not yet optimal.

As in the case of Hipparcos, the great success of the Gaia mission has now prompted scientists to think again about a follow-up astrometric space mission. Since Gaia observes in the optical range, it is reasonable to plan a high-precision astrometric infrared mission, which would make it possible to observe sources behind dust clouds and in the center of the Milky Way. However, such a possible infrared mission, which still has to be planned, developed and built, will not be able to provide scientific data for several decades at the earliest. Until then, the Gaia catalogues will remain the state of the art …

Literature

Antoja, T., Helmi. A., Romero-Gómez, M. (2018), A dynamically young and perturbed Milky Way, Nature 561, 360-362

Bastian, U. (2013), `Projekt Gaia: Die sechsdimensionale Milchstraße Teil 1, Sterne und Welt-raum 52, 36-44

Chandra, V., Semenov, V. A., Rix, H.-W., et al. (2023), The Three-Phase Evolution of the Milky Way, https://arxiv.org/pdf/2310.13050

Dehnen, W. (1999), The Pattern Speed of the Galactic Bar, The Astrophysical Journal, 524:L35-L38

Gaia Collaboration, Prusti, T., de Bruijne, J.H.J., et al. (2016a), The Gaia Mission, Astronomy and Astrophysics, 595, A1

Gaia Collaboration, Brown, A.G.A., Vallenari, A., et al. (2016b), Gaia Data Release 1: Summary of the astrometric, photometric, and survey properties, Astronomy and Astrophysics, 595, A2

Gaia Collaboration, Brown, A.G.A., Vallenari, A., et al. (2018), Gaia Data Release 2: Summary of the contents and survey properties, Astronomy and Astrophysics, 616, A1

Gaia Collaboration, Brown, A.G.A., Vallenari, A., et al. (2021), Gaia Early Data Release 3: Summary of the contents and survey properties, Astronomy and Astrophysics, 649, A1

Gaia Collaboration, Vallenari, A., Brown, A.G.A., et al. (2023), Gaia Data Release 3: Summary of the contents and survey properties, Astronomy and Astrophysics, 674, A1

Gaia Collaboration, Panuzzo, P., Mazeh, T., et al. (2024), Discovery of a dormant 33 solar-masses black hole in pre-release Gaia astrometry, Astronomy and Astrophysics, 686, L2

Helmi, A., Babusiaux, C., Koppelmam, H.H. et al. (2018), The merger that led to the formation of the Milky Way's inner stellar halo and thick disk, Nature 563, 85-88

Lindegren, L., Hernández, J., Bombrun, A., et al. (2018), Gaia Data Release 2: The astrometric solution, Astronomy and Astrophysics, 616, A2

Perryman, M. A. C., Lindegren, L., Kovalevsky, J. (1997), The Hipparcos Catalogue, Astronomy and Astrophysics, 323, L49-L52

Rix, H.-W., Chandra, V., Andrae, R., et al. (2023), The Poor Old Heart of the Milky Way, ApJ 941, 45

Shen, K. J., Boubert, D., Gänsicke, B.T., et al. (2018), Three Hypervelocity White Dwarfs in Gaia DR2: Evidence for Dynamically Driven Double-degenerate Double-detonation Type Ia Supernovae, The Astrophysical Journal, 865:15

Further Reading

Spatium N.16, O. Botta, Astrobiology 2006

Spatium N.28, M. Falanga, How Black are Black Holes? 2011

Spatium N.32, G. Meylan, Mirages in The Universe, 2013.

Spatium N.47, B. Leibundgut, Modern Cosmology – nearly perfect but incomplete, 2021.

The Author

Dr. Michael Biermann studied physics, astronomy and mathematics at the Ruhr University Bochum and the Ruprecht-Karls-University Heidelberg. In 2001, he obtained his PhD at the Institute of Theoretical Astrophysics in Heidelberg. After his doctorate, he became a scientific associate at the Heidelberg-Königstuhl State Observatory from 2001 to 2004, and since 2004 at the Astronomisches Rechen-Institut in Heidelberg, working on the astrometric satellite missions DIVA, AMEX and Gaia. For the ESA astrometric space mission Gaia, which was successfully launched in December 2013 and is in operations since July 2014, he was primarily responsible for the set-up, development, operations and maintenance of the First Look system, an essential tool for the daily assessment of the satellite status and the quality of the scientific data. Since 2016, he has been the head of the astrometric data reduction in the international Gaia consortium. He is also working group leader at the Astronomisches Rechen-Institut (ARI) of the Center for Astronomy of Heidelberg University (ZAH). With his group he is not only working on Gaia, but also on the preparation of the data reduction of the astrometric Japanese space mission JASMINE and on studies of digital satellite twins.

SPATIUM